Appl. Phys. B 34, 167–170 (1984)

Applied Physics B Photophysics and Laser Chemistry

Saturation Spectroscopy of Coherent Raman Scattering in Molecular Gases

V. N. Zadkov, N. I. Koroteev, M. V. Rychov, and A. B. Feodorov

Physics Department, Moscow State University, SU-117234 Moscow, USSR

Received 8 November 1983/Accepted 12 February 1984

Abstract. We present the theory of two-photon Raman saturation of a two-level Raman transition studied by an independent CARS process. The main goal here is to probe the saturated homogeneous Raman line shape. It is shown that there appears a saturation dip with a width determined by the relaxation time T_1. In the case of Doppler-broadened line the coherent Raman saturation spectroscopy may be used to determine both the T_1 and T_2 relaxation times.

PACS: 42.65 Cq, 33.80

Saturation absorption spectroscopy has become a powerful tool for studying Doppler-free electron absorption spectra [1, 2]. This work is devoted to the possible extrapolation of the saturation technique to the field of Raman-active transitions in the vibrational spectra of molecules.

Two intense pump waves are needed to saturate the transition under study, and the probing is to be carried out by coherent anti-Stokes Raman spectroscopy (CARS) [3, 4]. This problem has earlier been discussed in [5] and it has been solved there within the incoherent approximation taking into account only the population changes under the influence of biharmonic pump waves. It has been shown that a specific peculiarity appears in the center of the line with a width proportional to T_2^{-1}. However, the conclusions made in [5] are not accurate enough. It is necessary to take into account coherent effects, and most of all, the population oscillations in the two-level system [6].

This paper presents the calculation of the CARS signal line-shape carried out for the case of coherent effects. An additional narrow dip with the width proportional to T_1^{-1} is shown to appear in the CARS spectrum both in the cases of Doppler-broadened and homogeneously broadened lines.

1. Main Equations

The problem is considered within the approximation of a two-level system and fixed pump and probe fields. Equations for the populations difference n and the coherent amplitude Q of molecular vibrations are the following ones [3]:

$$\frac{dn}{dt}+\frac{n-1}{T_1}=-\frac{1}{2\hbar\Omega}\left(\frac{\partial\alpha}{\partial Q}\right)E^2\frac{dQ}{dt}, \tag{1}$$

$$\frac{d^2Q}{dt^2}+\frac{2}{T_2}\frac{dQ}{dt}+\Omega^2Q=\frac{1}{2M}\left(\frac{\partial\alpha}{\partial Q}\right)E^2n. \tag{2}$$

Here Ω is the frequency of the transition under study, T_1 and T_2 are the vibrational energy and phase relaxation times, respectively, $\alpha(Q)$ is a polarizability. The field E in (1 and 2) is a superposition of two pairs of plane waves, namely, a pair of pump waves with the frequencies ω_1 and ω_2 and a pair of probe waves with the frequencies ω_1' and ω_2'.

For the collinear interaction:

$$\mathbf{E}=\tfrac{1}{2}(\mathbf{A}_1\mathrm{e}^{-\mathrm{i}\omega_1 t}+\mathbf{A}_2\mathrm{e}^{-\mathrm{i}\omega_2 t}+\text{c.c.})+\tfrac{1}{2}(\mathbf{A}_1'\mathrm{e}^{-\mathrm{i}\omega_1' t}+\mathbf{A}_2'\mathrm{e}^{-\mathrm{i}\omega_2' t}+\text{c.c.}). \tag{3}$$

The steady-state solution of system of (1, 2) is assumed to have the following form:

$$Q=\tfrac{1}{2}Q_0\mathrm{e}^{-\mathrm{i}(\omega_1-\omega_2)t}+\tfrac{1}{2}Q_0'\mathrm{e}^{-\mathrm{i}(\omega_1'-\omega_2')t}+\text{c.c.}, \tag{4}$$

$$n=n_0+\tfrac{1}{2}\tilde{n}_0\mathrm{e}^{-\mathrm{i}[(\omega_1-\omega_2)-(\omega_1'-\omega_2')]t}+\text{c.c.}, \tag{5}$$

where $\omega_1-\omega_2\approx\Omega\approx\omega_1'-\omega_2'$. Let

$$\Delta=[(\omega_1-\omega_2)-\Omega]T_2,\ \Delta'=[(\omega_1'-\omega_2')-\Omega]T_2$$

and

$$G=\frac{T_1T_2|A_1A_2|^2}{16M\hbar\Omega}\left(\frac{\partial\alpha}{\partial Q}\right)^2,\quad g=\frac{T_1T_2|A_1'A_2'|^2}{16M\hbar\Omega}\left(\frac{\partial\alpha}{\partial Q}\right)^2,$$

(saturation parameters for pump and probe waves, respectively).

From (2–5) the expressions for the coherent amplitudes result in

$$Q_0=\frac{T_2}{4M\Omega}\left(\frac{\partial\alpha}{\partial Q}\right)\frac{n_0A_1A_2^*+\frac{\tilde{n}_0}{2}A_1'A_2'^*}{-\mathrm{i}-\Delta},\tag{6}$$

$$Q_0'=\frac{T_2}{4M\Omega}\left(\frac{\partial\alpha}{\partial Q}\right)\frac{n_0A_1'A_2'^*+\frac{\tilde{n}_0}{2}A_1A_2^*}{-\mathrm{i}-\Delta'}.\tag{7}$$

It is easy to obtain three complex linear equations for n_0, $\tilde{n}_0$, $\tilde{n}_0^*$ which may be reduced to the real equations by the following substitution:

$$\begin{aligned}\tilde{n}_0&=\tilde{n}_0'+\mathrm{i}\tilde{n}_0'',\\ \tilde{n}_0^*&=\tilde{n}_0'-\mathrm{i}\tilde{n}_0''.\end{aligned}\tag{8}$$

We make the same substitution in (7) and calculate Q_0. The third-order nonlinear susceptibility $\chi^{(3)R}$ is proportional to Q_0', leading to

$$\begin{aligned}I_{\mathrm{CARS}}&\sim|\chi^{(3)R}|^2\\&=(\tilde{\chi}^{(3)R})^2\frac{\left(2n_0+\sqrt{\frac{G}{g}}\tilde{n}_0'\right)^2+\left(\sqrt{\frac{G}{g}}\tilde{n}_0''\right)^2}{\Delta'^2+1},\end{aligned}\tag{9}$$

where

$$\tilde{\chi}^{(3)R}=\frac{NT_2}{48M\Omega}\left(\frac{\partial\alpha}{\partial Q}\right)_0^2,\tag{10}$$

N being the number of molecules in the unit volume.

Expression (9) shows that the CARS signal line profile depends both on the static population difference change n_0 and optical nutations caused by the terms proportional to $\tilde{n}_0'$ and $\tilde{n}_0''$. We do not write down the closed-form analytical solution of (9) because of it is cumbersome. However, the general analytical solution of (9) can easily be analysed numerically and the CARS signal lineshape can be calculated exactly for arbitrary values of g/G and T_1/T_2 ratios.

When $g/G\ll1$ rather simple analytical expression for $I_{\mathrm{CARS}}(\Delta')$ can be obtained. In this case the solution of the problem is to be searched in the form of a perturbation-theory expansion series based on a small parameter g/G. Assuming that $|Q_0'|\ll|Q_0|$, $|\tilde{n}_0|\ll|n_0|$ and leaving only the terms of the first order of smallness, i.e. proportional to g/G, we obtain the following equations which are analogous to (6–7):

$$Q_0=\frac{T_2}{4M\Omega}\left(\frac{\partial\alpha}{\partial Q}\right)\frac{n_0A_1A_2^*}{-\mathrm{i}-\Delta},\tag{11}$$

$$Q_0'=\frac{T_2}{4M\Omega}\left(\frac{\partial\alpha}{\partial Q}\right)\frac{n_0A_1'A_2'^*+\frac{\tilde{n}_0}{2}A_1A_2^*}{-\mathrm{i}-\Delta'}\tag{12}$$

as well as the expressions for n_0 and $\tilde{n}_0$:

$$n_0=\frac{1}{1+\frac{G}{1+\Delta^2}},\tag{13}$$

$$\begin{aligned}&\left[1+\mathrm{i}(\Delta-\Delta')\frac{T_1}{T_2}-\mathrm{i}\frac{G/2}{-\mathrm{i}-\Delta'}\right]\tilde{n}_0^*\\&\quad=n_0\left(\frac{\mathrm{i}\sqrt{Gg}}{-\mathrm{i}-\Delta'}-\mathrm{i}\frac{\sqrt{Gg}}{\mathrm{i}-\Delta}\right).\end{aligned}\tag{14}$$

Substituting (13, 14) into (12) we obtain for the coherent amplitude Q_0':

$$\begin{aligned}Q_0'=\frac{T_2}{4M\Omega}\left(\frac{\partial\alpha}{\partial Q}\right)&\frac{-1}{1+\frac{G}{1+\Delta^2}}\\&\cdot\frac{1+\mathrm{i}(\Delta-\Delta')\frac{T_1}{T_2}-\frac{\mathrm{i}G/2}{\mathrm{i}-\Delta}A_1'A_2'^*}{1+\mathrm{i}(\Delta-\Delta')\frac{T_1}{T_2}+\frac{\mathrm{i}G/2}{\mathrm{i}+\Delta'}}.\end{aligned}\tag{15}$$

The resulting expression for I_{CARS} is

$$\begin{aligned}I_{\mathrm{CARS}}\sim\frac{|\chi^{(3)R}|^2}{(\tilde{\chi}^{(3)R})^2}&=\frac{4}{\left(1+\frac{G}{1+\Delta^2}\right)^2}\\&\cdot\frac{\left(1-\frac{G/2}{1+\Delta^2}\right)^2+\left[(\Delta-\Delta')\frac{T_1}{T_2}+\frac{\Delta G/2}{1+\Delta^2}\right]^2}{\left[\Delta'-(\Delta-\Delta')\frac{T_1}{T_2}\right]^2+\left[\Delta'(\Delta-\Delta')\frac{T_1}{T_2}+1+\frac{G}{2}\right]^2}.\end{aligned}\tag{16}$$

2. The Homogeneous CARS Signal Lineshape Analysis

The calculations have shown that the general solution of (9) and the perturbation theory solution (16) are the same when $g/G\lesssim0.1$, $g\ll1$.

Figure 1 illustrates the influence of the saturation parameter G on the lineshape of the CARS signal in the case of a homogeneously broadened Raman transition. The spectral line is clearly seen to have a purely Lorentzian profile in the absense of pump waves ($G=0$). The increase of G leads to the formation of a

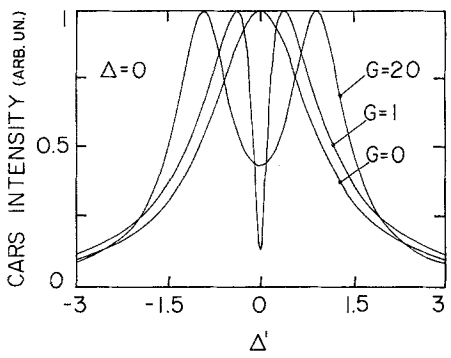

Fig. 1. The deformation of the homogeneous CARS signal lineshape due to the saturation effect by independent biharmonic Raman pumping for various values of the saturation parameter G: 0; 1; 20 $\Delta'=(\omega_1'-\omega_2'-\Omega)T_2$

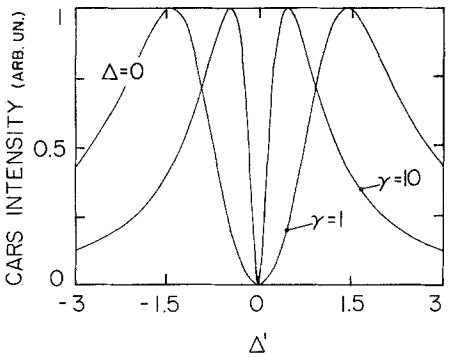

Fig. 2. The illustration of the dependence of the dip width in the saturated CARS signal lineshape upon time T_1 (homogeneously-broadened Raman transition): $\gamma=T_1/T_2=1$ and 10; $G=2$

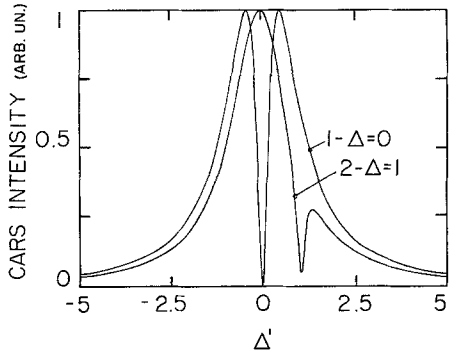

Fig. 3. The lineshape of saturated homogeneous CARS-signal spectral profile for various values of Δ: *1* $\Delta=0$; *2* $\Delta=1$. $T_1/T_2=10$, $G=2$

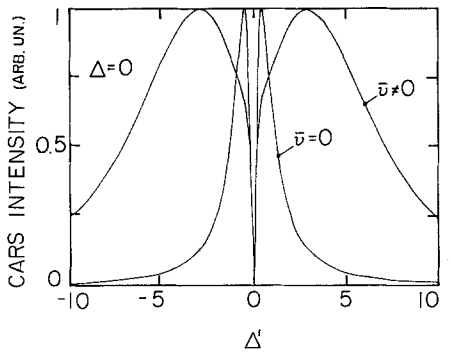

Fig. 4. The lineshape of Doppler-broadened saturated CARS signal band profile for various gas temperatures: *1* $T\simeq 0(\mathfrak{v}=0)$; *2* $T\simeq 300\,\mathrm{K}(\mathfrak{v}\neq 0)$. $T_1/T_2=10$; $G=2$

dip, the depth of which grows with the increase of G and reaches the maximum value at $G=2$. With G grows further, the dip depth lessens and the frequency interval between the two maxima in the profile of the $I_{\mathrm{CARS}}(\Delta')$ lineshape increases.

As one can see in Fig. 2, the width of the dip is proportional to T_1^{-1}. It means that the dip appears due to the processes of population changes, since T_1 is nothing but the characteristic time of these changes (compare with the results of [6]).

In our case the oscillations of the population difference with the frequency $\Delta-\Delta'$ [terms with $\tilde{n}_0$ and $\tilde{n}_0^*$ in (5)] modulate the net population difference with the same frequency. When Δ' tends to Δ the frequency of population oscillations decreases and the index of the modulation increases. At $\Delta'=\Delta$ we obtain the deepest hole in the homogeneous CARS signal line profile, the width of which is $\sim T_1^{-1}$.

Figure 3 illustrates the influence of pump-wave detuning Δ on the line profile of the "saturated" CARS signal. With Δ detuning off resonance the dip shifts from the center of the line.

3. The Doppler-Broadened Saturated CARS Lineshape Analysis

The results obtained above can be generalized to the case of an inhomogeneously broadened line and, in particular, to a Doppler-broadened one. For this purpose it's necessary to make the following substitution in (9), or (16):

$$\Delta\to\Delta-(\mathbf{k}_1-\mathbf{k}_2)\mathfrak{v}T_2,$$

$$\Delta'\to\Delta'-(\mathbf{k}_1'-\mathbf{k}_2')\mathfrak{v}T_2,$$

where $\mathfrak{v}$ is a vector of the thermal-motion velocity of a molecule under study, and then to integrate the expression obtained over $\mathfrak{v}$ using the Maxwell distribution of molecular velocities.

We do not write out the general analytical solution obtained following this scheme because it is cumbersome, too. The results of computer calculations for different values of thermal velocities of molecules are represented in Fig. 4. The obvious consequence of the thermal-velocity distribution is the broadening of the spectral line. The profile of the dip, however,

changes in a more complicated manner: now it consists of the two holes (one inside another) with characteristic widths proportional to T_2^{-1} and T_1^{-1}, respectively. Thus the coherent saturation spectroscopy of Raman transitions provides a possibility for simultaneous measurements of both T_1 and T_2 times.

Both the existence and depth of the saturation dip proportional to T_1^{-1} strongly depend on the geometry of the interaction of the light waves. The picture just drawn (Fig. 4) are relevant for the case of co-directional propagation of the pumping and probing waves. In the opposite case of counter-propagating pumping and probing waves the saturation dip with the width $\sim T_1^{-1}$ vanishes and that with the width $\sim T_2^{-1}$ survives. It is the last dip that has been experimentally detected by Owyoung and Esherick [7] in a Doppler-broadened $Q_{01}(2)$ Raman line in deuterium gas. However, they were unable to detect the much narrower saturation dip with the width $\sim T_1^{-1}$ in a co-directional geometry because of the lack of the needed very high spectral resolution.

4. Discussion

The results obtained above allow one to consider the coherent saturation spectroscopy as a method for determining the relaxation times T_1 and T_2. In order to evaluate the real parameters of lasers needed to perform the saturation CARS experiment, let us consider the typical Raman transition, the single rotational transition $S_0(1)$ in the hydrogen gas ($T_1 = 0, 1\,\mu s$, $T_2 = 2\,ns$ at $p = 1\,atm$).

According to [8] the saturation parameter value $G \approx 10$ can easily be achieved when experimenting with the Raman line. This value G is more than enough to observe the discussed effects since the maximum depth of the hole occurs at $G = 2$ (in this case the laser powers needed are about $P_1 = 1\,MW$, $P_2 = 100\,kW$). The width of the dip $\sim T_1^{-1}$ is $\Delta\omega$ (FWHM) $\sim 0.0002\,cm^{-1}$ and the homogeneous linewidth is $\Delta\omega_{hom}$ (FWHM) $\sim 0.0009\,cm^{-1}$, which is proportional to T_2^{-1}. At the same time the Doppler width of the line is $\Delta\omega_d = 0.005\,cm^{-1}$.

The spectral resolution (less then or equal to $0.0002\,cm^{-1}$) needed to detect both T_1 and T_2 from the profile of the Doppler-broadened $S_0(1)$ line in hydrogen gas can be obtained with the use of a pulsed amplifier chain of a stabilized cw dye laser output, developed by Drell and Chu [9] and by Owyoung [7, 10].

It is clear, however, that there exists an opportunity of using the time-domain-spectroscopy technique instead of the frequency-domaine one, as it does in every other nonlinear spectroscopy scheme [3].

In this particular case one should detect the dependence of the intensity of the CARS signal on the delay time between saturating and probing pulses, the period of fast oscillations in this dependence giving the relaxation time T_2 and the decay time giving the relaxation time T_1. For our example of the $S_0(1)$ line in H_2 gas the delay time needed should be less than or equal to $\sim 1\,\mu s$, and the pulse durations should be shorter than or equal to 100 ps.

In conclusion, we should like to point out some possible applications of the predicted saturation dip with the width $\sim T_1^{-1}$. The gas cell with the saturated Raman line can be used inside the laser cavity as a frequency narrowing and stabilizing element in the same manner as an ordinary Lamb-dip saturation cell is used for the same purposes. The difference is that the width of the Raman saturation dip $\sim T_1^{-1}$ can be made much narrower than the Lamb absorption dip can ($\sim T_2^{-1}$) if the widths of saturating fields in the Raman cell are sufficiently narrow ($\Delta\nu_{1,2} \lesssim T_1^{-1}$).

Acknowledgements. The authors would like to gratefully acknowledge helpful discussions with S.A. Akhmanov, A.I. Burshtein, S.M. Gladkov, and S. Yu. Nikitin.

References

1. V.S. Letokhov, V.P. Chebotaev: *Nonlinear Laser Spectroscopy*, Springer Ser. Opt. Sci. **4** (Springer, Berlin, Heidelberg, New York 1975)
2. S.G. Rautian, G.I. Smirnov, A.M. Shalagin: *Nonlinear Resonanses in the Spectra of Atoms and Molecules* (Nauka, Novosybirsk 1979)
3. S.A. Akhmanov, N.I. Koroteev: *Methods of Nonlinear Optics in Light Scattering Spectroscopy* (Nauka, Moscow 1981)
4. A. Weber (ed.): *Raman Spectroscopy of Gases and Liquids*, Topics Current Phys. **11** (Springer, Berlin, Heidelberg, New York 1979)
5. D.N. Kozlov, V.V. Smirnov, V.I. Fabelinskii: Sov. Phys. Dokl. **24**, 369 (1979)
6. E.V. Baklanov, V.P. Chebotaev: Sov. Phys. JETP **60**, 552 (1971)
7. A. Owyoung, P. Esherick: Opt. Lett. **5**, 421 (1980)
8. A.M. Brodnikovsky, V.N. Zadkov, M.G. Karimov, N.I. Koroteev: Opt. Spektrosk. **54**, 385 (1983)
9. P. Drell, S. Chu: Opt. Commun. **28**, 343 (1979)
10. A. Owyoung: In *Laser Spectroscopy* IV, ed. by H. Walther, K.W. Rothe, Springer Ser. Opt. Sci. **21** (Springer, Berlin, Heidelberg, New York 1979) p. 175